

Rosetta Navigation during the End of Mission Phase

By Pablo MUÑOZ,¹⁾ Vicente COMPANYS,²⁾ Frank BUDNIK,²⁾ Bernard GODARD,³⁾
Dario PELLEGRINETTI,¹⁾ Gabriele BELLEI,⁴⁾ Rainer BAUSKE,⁵⁾ and Waldemar MARTENS²⁾

¹⁾GMV at ESOC, Darmstadt, Germany

²⁾ESA/ESOC, Darmstadt, Germany

³⁾Telespazio Vega at ESOC, Darmstadt, Germany

⁴⁾Deimos Space at ESOC, Darmstadt, Germany

⁵⁾Terma at ESOC, Darmstadt, Germany

(Received June 21st, 2017)

ESA's Rosetta mission ended on 30th September 2016, after 26 months of operations around the comet 67P/Churyumov-Gerasimenko to characterize it, deploy the Philae lander on its surface, and monitor its evolution during the perihelion passage. The date selected for Rosetta End of Mission (EoM) was immediately before entering superior solar conjunction and at a point in the heliocentric orbit where the increasing distance to both Sun and Earth was already imposing major constraints on the scientific operations, due to limited solar power received on board and downlink data rate. The last two months of Rosetta operations were dedicated to fulfil the high-level mission objective of orbiting the comet as low as possible and terminating the mission with a direct descent and slow impact on the comet's surface. Flying so close to the comet was extremely challenging for navigation due to the strong orbital perturbations from the gravitational field of such an irregular body. This phase is considered a success and very fruitful in terms of scientific return. Moreover, it was during this period that the lander search campaign finally succeeded to image Philae at rest on its landing site. This paper describes the trajectory design for the EoM scenario, it discusses the encountered navigation challenges and how they were tackled, and it reports the achieved navigation results.

Key Words: Rosetta, small body navigation, trajectory design, low flyovers, controlled impact

1. Introduction

Rosetta was an interplanetary cornerstone mission in ESA's long-term space science program. Its main objective was the exploration and study of comet 67P/Churyumov-Gerasimenko during its approach to the Sun. The spacecraft carried 11 scientific instruments and a lander module, Philae, with 10 additional instruments, for the most detailed study of a comet ever performed.

Launched in March 2004 with an Ariane-5/G1, it used 4 planetary swingbys (Earth ¹⁾ and Mars ²⁾) to obtain the required velocity to reach the orbit of the comet. During its long journey, Rosetta had close encounters (flybys) with 2 asteroids: (2867) Šteins ³⁾ and (21) Lutetia ⁴⁾. Rosetta arrived at the comet 67P on August 6th 2014.⁵⁾ On November 12th 2014, Rosetta successfully delivered the lander Philae into its descent trajectory to the selected landing site on the comet's surface.⁶⁾ Afterwards, Rosetta continued its scientific mission, escorting the comet through its perihelion passage (August 2015), studying its activity evolution during its approach to the Sun and along its way back to the outer Solar system.

Due to the increased comet activity around perihelion, the number of dust particles lifted by the ejected gas increased dramatically during 2015. This originated the risk of Rosetta's star trackers getting confused by the number of "false" stars and the higher background signal in the sensors. During the 6-km altitude flyby in February 14th 2015, the star trackers lost track for a few hours, while one month later, on March

28th, during a 13-km altitude flyby, they lost track again and were out of the control loop for about 24 hours, ultimately leading to a spacecraft safe mode. To mitigate this risk, the performance of the star trackers (background level, number of false stars) had to be assessed at each planning cycle. Whenever it was detected that the star tracker performance was close to the limit, the distance from the spacecraft to the comet was increased, as shown in Fig. 1. It was only well after perihelion that the comet activity started to decrease, thus allowing to bring the spacecraft closer to the comet again.

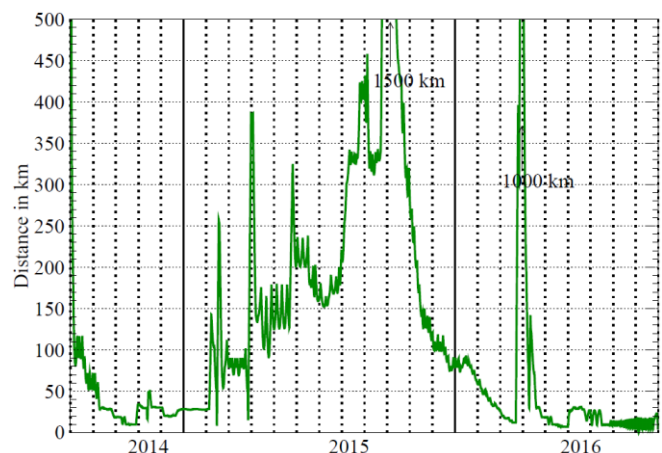


Fig. 1. Distance from Rosetta to the comet from Aug 2014 to Sep 2016. Out of the scale are the 1500 km distance of the "far excursion" in October 2015 and the 1000 km of the "tail excursion" in April 2016.

2. End of Mission Scenario

Rosetta's nominal end of mission was originally planned for end of 2015. Since the spacecraft platform and the scientific instruments were in good health, the mission was extended by 9 months, until end of September 2016, when Rosetta would be 4.0 au (astronomical units) from the Sun and 4.7 au from the Earth. The mission was not extended further because, in October 2016, the spacecraft would have entered in superior solar conjunction, thus interrupting normal operations and, after the conjunction, it would have been so far away from the Sun that the reduced solar power received on board would not have been sufficient to support the essential spacecraft subsystems.

It was decided that in August and September 2016, during the so-called End of Mission phase (EoM), the spacecraft would be flown at very low altitudes (flyovers), allowing for scientific observations of unprecedentedly high resolution, and terminate the mission with a slow descent towards a gentle impact on the comet's surface,⁷⁾ although the spacecraft had not been designed for landing. This way, Rosetta would follow a similar fate to NASA's NEAR Shoemaker mission. In 2001, after one year of studying the asteroid Eros, NEAR performed a series of low altitude flybys, followed by a controlled descent, soft landing, and, remarkably, remained operational for 16 days at rest on the asteroid's surface.⁸⁾

In the case of Rosetta, it would not have been possible to operate the spacecraft after the impact on the comet's surface, despite the even lower impact velocity (about half the speed of NEAR's). At such high geocentric distance (4.7 au) the only possible communication method with ground was via Rosetta's High Gain Antenna (HGA), whose half beam width was about 0.5 deg. Due to the irregular shape of the comet, it was extremely unlikely that, after landing, the spacecraft would remain within half a degree of the targeted attitude. Even in that remote case, the comet rotation would very quickly drift away the antenna from Earth-pointing and interrupt communications. To ensure proper spacecraft passivation, an on-board sequence was prepared and uplinked in advance, so that the spacecraft would autonomously switch off all its subsystems immediately after touchdown and disable any possible reboot of its on-board computer.⁹⁾

The EoM scenario was very challenging in terms of trajectory design, navigation and planning. Navigation during the EoM was expected to be more difficult than any previous mission phase, including Philae's delivery. The following sections describe the trajectory design, navigation challenges and results obtained in each sub-phase of the Rosetta EoM scenario.

3. Low Circular Orbits

3.1. Description

During the early design of the Rosetta EoM scenario, it was conceived that the first stage should consist of circular orbits with the smallest possible radius. Up to that time the closest that Rosetta had orbited the comet had been at ~10 km radius, in October 2014, during the Close Observation phase immediately before Lander Delivery.⁶⁾ Afterwards, the spacecraft had to be flown at larger distances due to the much higher activity of the comet. After perihelion, the comet

activity started to decrease and the distance from the spacecraft to the comet was reduced down to 12 km distance in March 2016, before the transition to the tail excursion.

Having low quasi-circular orbits during an extended period of time was considered a prerequisite for the flyover phase, since they would allow to refine the estimation of the gravitational field of the comet and build a denser set of higher resolution landmarks (local surface maps used for optical navigation), both required for accurate navigation during the flyovers. Once the long term scientific plan for 2016 was defined, it was noted that it included an extended period of time in May 2016 with the high-level requirement of flying "ACAP" (as close as possible) terminator orbits. It was therefore proposed and agreed that, assuming the comet activity would allow for it, the low circular orbits would be flown in May, accomplishing this phase before the proper EoM phase started. Advancing this phase posed an additional challenge because the performance of the star trackers had to be carefully assessed since the comet activity in May would be significantly higher than in August.

3.2. Trajectory Design

The orbits flown in this phase (Fig. 2) were defined in the day/night terminator plane (the plane containing the comet centre and perpendicular to the Sun direction), i.e. dawn-dusk orbits. This type of orbits has certain advantages for navigation: (1) the navigation images are all taken at similar illumination conditions, from 90 deg phase angle (Sun-comet-probe angle), ensuring that enough landmarks could be identified in all images; (2) in this geometry, the spacecraft solar arrays are edge-on with respect to the incoming flow of the outgassing comet, thus minimizing the drag force.

This phase was planned to start with the spacecraft in a 10-km terminator orbit. The main design drivers were: (1) keep the regular operations pattern: planning cycles on Mondays and Thursdays, manoeuvres on Wednesdays and Sundays; and (2) reduce the orbit radius in steps so that, in case of star tracker contingency, the apocentre of the orbit would still be in an altitude region considered safe.

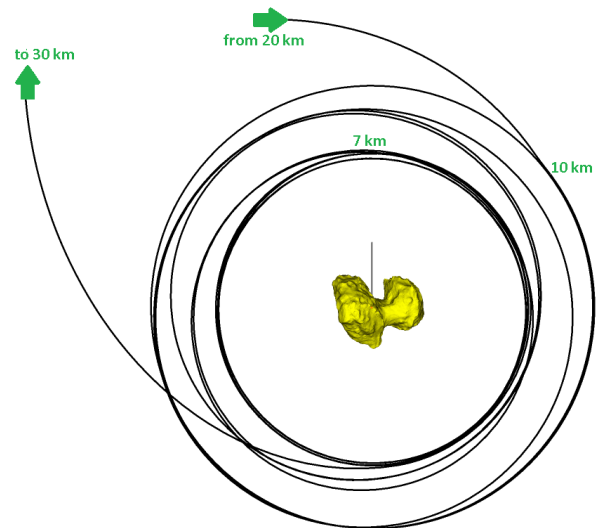


Fig. 2. Low quasi-circular orbits flown in May 2016.

Given that the scheduling pattern was fixed, having one manoeuvre every 3-4 days, it was not possible to use Hohman transfers because the manoeuvres occurred anywhere along the orbit, not necessarily at pericentre or apocentre. Therefore, an ad-hoc solution had to be found in which each manoeuvre was progressively reducing simultaneously the apocentre and pericentre radii. Once the final 7-km orbit was acquired, no deterministic orbit control manoeuvres were planned during a period of 7 days. This was considered beneficial for the subsequent estimation of the gravitational field based on the data collected during this phase.

The full list of manoeuvres and orbits flown in this period is given in Table 1, including the transition to the subsequent 30-km mapping phase that, analogous to the Global Mapping phase in 2014,¹⁰⁾ consisted of two half orbits with 45-degree tilt with respect to the terminator plane.

Table 1. List of manoeuvres and orbit sizes designed for May 2016.

Date	Manoeuvre Slot		Resulting orbit radius [km]	
	Time UTC	ΔV [cm/s]	Apocentre	Pericentre
05/11	01:40	5.8	10.0	10.0
05/15	01:40	1.2	10.0	8.5
05/18	13:40	2.5	9.0	7.5
05/22	01:40	2.5	8.0	7.0
05/25	01:40	2.1	7.0	7.0
05/29	01:40	unused	7.0	7.0
06/01	01:40	8.7	29.0	7.0

3.3. Navigation Results

In terms of navigation this phase was flown very accurately. Despite the lower altitudes flown, the optical navigation system had no problems in identifying landmarks and the gravitational field model used at that time was good enough to ensure sufficient navigation accuracy.

No significant star trackers problems were identified in the stepping down period, nor in the first couple of revolutions of the final 7-km orbit. However, on Saturday May 28th, in the middle of the 7-day arc, the star trackers suddenly lost track and were not able to re-acquire again, leading to a very critical situation for the mission in which the spacecraft was in safe-mode without absolute attitude measurements and, due to the consequent attitude de-pointing, no signal was received on ground for about 24 hours.¹¹⁾ Critical actions had to be performed attempting to recover the spacecraft including commanding in the blind. Fortunately, it was successfully brought to normal mode and commanded to capture new navigation images so that the navigation knowledge could be regained, just in time for the commanding of the manoeuvre planned to start the transition to the 30-km orbits.

These low circular orbits were very valuable from a scientific point of view, especially for the ROSINA instrument,¹²⁾ that was able to detect, for the sole time in the whole mission, the presence of Krypton and Xenon in the comet environment.¹³⁾ This phase was also very relevant to establish the basis for accurate navigation during the flyover phase. The images from the navigation cameras (NAV CAMs) taken during these 7-10 km orbits, at 90 deg phase angle, were combined with the ones from the scientific narrow angle camera, OSIRIS-NAC¹⁴⁾ (equivalent resolution at 5 times the

distance), taken during the mapping phase, at 30 km and 45-90 deg phase angle, to build a new set with more than 10,000 high-resolution landmarks defined on the whole comet's surface. Ref. 15-17) describe in detail the techniques for Rosetta's navigation image processing. Additionally, the optical and radiometric data accumulated during this phase (up to the safe-mode) were very useful to obtain more accurate estimations of the comet's gravitational field both in preparation of and during the flyover phase.¹⁸⁾

4. Flyover Orbits

4.1. Description

The main scientific objective of this phase was to fly as close as possible to the comet's surface over extended periods of time taking scientific observations of unprecedentedly high resolution. Flying so close to the comet was very challenging for navigation because: firstly, the optical navigation (essential for orbit determination around the comet) had to identify sufficient landmarks in each navigation image taken at altitudes never flown before; and secondly, flying at such a low altitude subjects the spacecraft to strong orbital perturbations due to the gravitational field of such an irregular body. Accurately modelling this perturbation is, in the case of the comet, not an easy task, and even harder given that there was no previous navigation experience at such low altitudes.

4.2. Trajectory Design

The main drivers considered in the trajectory design were: 1) fly at the lowest possible altitudes over the comet surface ensuring scientific observations of well illuminated areas; 2) achieve a sufficiently accurate orbit predictability such that the commanded spacecraft pointing profile succeeded to point the scientific instruments and navigation camera to the desired target areas; 3) have a fixed repetitive pattern for spacecraft operations and scientific observations, so that the planning is defined at absolute times, independently of the actual trajectory that was flown; 4) keep planning cycles during daytime (normal working hours) but, for this phase, including weekends; 5) allocate enough time to acquire navigation images and tracking data after manoeuvres and pericentres so that the navigation knowledge could always be recovered even in case of significant manoeuvre misperformance or acute mismodelling of the gravitational perturbation around pericentre.

To keep the fixed pattern in absolute times, an orbital period of 3 days was chosen, so that all pericentres would occur at the same time of day. The orbital plane was chosen to have a tilt of 20 deg with respect to the terminator plane, placing the pericentre in the point of smallest phase angle (70 deg). Having a moderate tilt increased the chances of flying over illuminated areas around pericentre while preventing the apocentre from being too deep in the night side of the comet. It was essential for orbit determination that the navigation images around apocentre captured an illuminated fraction of the comet surface.

Figures 3 and 4 illustrate the adopted design. The trajectory consisted of a series of 15 elliptic orbits, called flyover orbits, with progressively decreasing pericentre radius, so that the

knowledge obtained in previous flyovers could be used to improve the navigation accuracy of the subsequent ones.

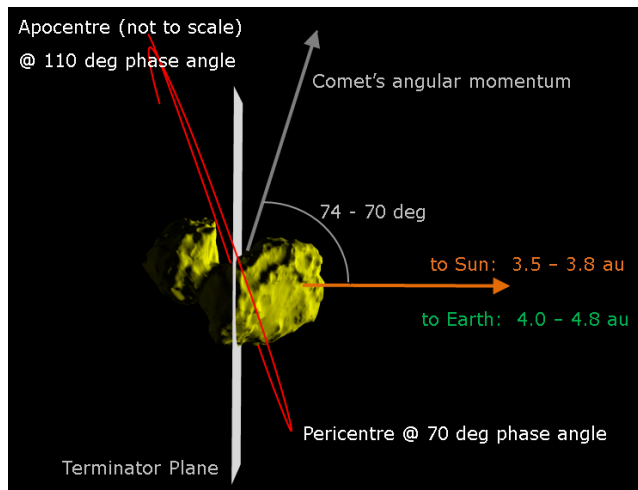


Fig. 3. Geometry sketch during the flyover orbits, prepared during the initial stages of the trajectory design. The values given in intervals correspond to the beginning and end of the EoM phase. The apocentre is not to scale (too close to the comet). The final selection of the orbital plane for the flyover phase (pericentre at 20 deg latitude) corresponds in this figure to a rotation of the orbit by about -105 deg around the Sun line.

Retrograde sense of orbital motion was preferred over prograde in order to mitigate the strong gravitational perturbations around pericentre. The combination of 3-day orbital period and 12.055 hours of comet's rotation period meant that consecutive flyovers would, nominally, be separated by 10 deg in longitude, thus achieving a reasonable surface coverage during the 15 planned flyovers. The repetitive geometry had the advantage that the experience obtained in previous flyovers is applicable to the next ones.

With this geometry definition, there is one additional degree of freedom that corresponds to a rotation of the orbit around the Sun direction (see Fig. 3). This choice would define the latitude and solar local time of pericentre and it was based on the inputs from the scientific teams: preference to observe different regions at each pericentre (maximized with the pericentre at the equator) and to fly over the northern hemisphere in the morning side of the comet, where the raising activity due to night-to-day transition could be observed. Additionally, it was noted that the points of the comet nucleus farther away from its centre of mass (CoM) are located in equatorial latitudes, and therefore flying over those points would imply lower altitude over the surface for the same pericentre radius. Considering all this, it was proposed and agreed to have pericentres at a latitude of 20 degrees north in the morning side of the comet, which corresponded to a solar local time of about 7 hours.

Figure 4 illustrates the trajectory pattern for each flyover orbit. To have full control over all orbital elements, two deterministic Orbit Control Manoeuvres (OCMs) were planned per orbital revolution, 12 hours before and after nominal pericentre time. In between manoeuvres, there was a period of about 20 hours around pericentre fully dedicated to scientific and navigation observations.

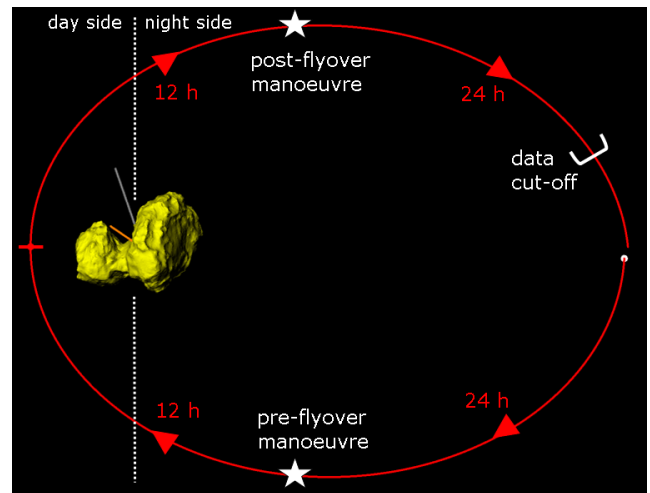


Fig. 4. Trajectory pattern for each flyover orbit.

One planning cycle per revolution was performed, while the spacecraft was flying around apocentre, based on an orbit determination with data cut-off 19 hours after the post-flyover manoeuvre, so that enough tracking and optical data was collected to regain the navigation knowledge after the gravitational perturbations around pericentre and the misperformance of the post-flyover manoeuvre.

4.3. Planning Cycles

Every three days, a Flight Dynamics (FD) planning cycle was performed on ground, consisting of the following steps: (1) processing of the latest navigation images for landmarks identification; (2) orbit determination based on radiometric and optical data; (3) optimization of the manoeuvres to be commanded and trajectory prediction; (4) generation of AOCS commands including the spacecraft attitude profile to point to target areas, selected by their predicted illumination conditions. The time allocated for the FD process was 12 hours. Once the FD commands were ready and checked, they were delivered to the Flight Control team that included other spacecraft and payload commands and sent them to the ground stations for uplink (for redundancy, two uplink opportunities from different ground stations were allocated).

Table 2. Summary of events per flyover orbit.

Time (UTC)		Event	
	06:40	on-board	Start of current commanded period
	09:00	on-board	Pre-flyover manoeuvre
	21:00	on-board	Pericentre (nominal time)
(+1d)	09:00	on-board	Post-flyover manoeuvre
(+2d)	04:00	on-board	OD data cut-off
(+2d)	05:00	on-ground	Reception of all navigation images
(+2d)	06:00	on-ground	Beginning of FD planning cycle
(+2d)	09:00	on-board	Apocentre (nominal time)
(+2d)	18:00	on-ground	Delivery of FD commands (latest)
(+2d)	22:00	on-ground	Availability of all commands at the ground station for uplink (latest)
(+3d)	06:40	on-board	Start of new commanded period

Table 2 lists a summary of the on-board and on-ground events per flyover revolution, while Figure 5 shows a sketch of the spacecraft operations timeline per revolution and the duration of each slot. Except during OCM slots, one

navigation image per hour was scheduled. Three Wheel-Off-Loading manoeuvres (WOLs) were performed per revolution, one around apocentre and the other two immediately before the manoeuvres. As it was beneficial for the orbit determination accuracy, the 19h arc immediately before data cut-off was left free of OCMs and WOLs. Another consideration was to ensure that the HGA could be continuously pointing to Earth in the periods for downlinking the navigation images (between post-flyover manoeuvre and data cut-off) and for uplinking the new commands that had to arrive on board before the first execution time (06:40).

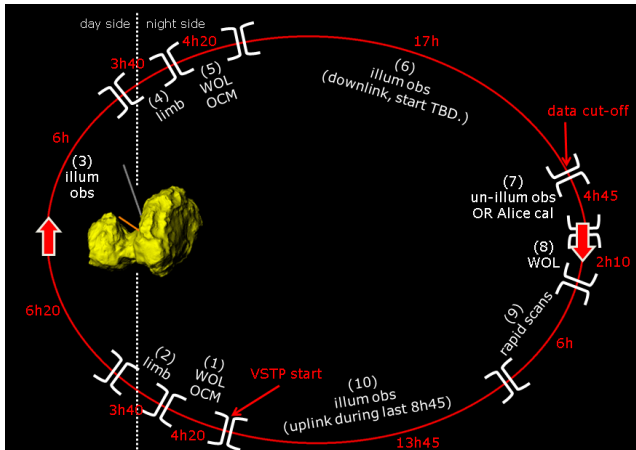


Fig. 5. Spacecraft timeline pattern per flyover orbit.

4.4. Gravitational Perturbations

The greatest navigation challenge in orbiting so close to the comet came from the strong orbital perturbations at each pericentre pass due to the extreme irregularity of the comet's gravitational field and the comet rotation. All orbital elements were perturbed by this effect, with the sole exception of the pericentre radius that experienced minor variations. At each planning cycle, the perturbations during the upcoming flyover had to be accurately predicted in order to pre-compensate them with the two commanded manoeuvres. The most sensitive and critical element was the resulting orbital period after each flyover. The magnitude and sign of variation of the orbital period strongly depends on the actual flight path followed by the spacecraft during the flyover. The error in the prediction of the orbital period leads to a linearly increasing orbit phasing error, thus an error in pointing to the comet, and shifts the subsequent pericentre time away from its nominal time, which could affect the planning scheme that was based on absolute times.

The stronger effect was experienced in flyover#8 (see section 4.7), with pericentre at 4.05 km from the comet's centre (about 1.5 times the comet's radius), in which the gravitational perturbation induced a variation in the orbital period of 19 hours. As an interesting comparison, the same type of perturbation is, at the time of writing this paper, being experienced by ExoMars-TGO around Mars at the beginning of its aerobraking operations.¹⁹⁾ In TGO's eccentric orbit, with 24h of orbital period and a pericentre radius of less than 1.04 times Mars' radius, the maximum variation of orbital period due to gravitational perturbation at pericentre is 1 minute.

The comet's gravitational field model used in operations for both orbit determination and manoeuvre optimization was a spherical harmonic expansion up to degree and order 5, with coefficients that were periodically re-estimated as more data from the flyovers was accumulated.¹⁸⁾ Another model was available, the so-called polyhedron gravitational model,²⁰⁾ that computes the gravitational field from a shape model,²¹⁾ under the assumption of constant density. This model could not be used in operations as it is much heavier in computation time and it does not allow for a simple parameterization that could be used in the estimation process. However, it was useful for analysis purposes, e.g., the assessment of how well the truncated spherical harmonic expansion captured the gravitational perturbations from a more complex model.

4.5. Orbit Determination

Rosetta OD was performed using the ESOC Interplanetary Orbit Determination System,²²⁾ enhanced to support simultaneous estimation of comet orbit, comet attitude and Rosetta orbit using radiometric tracking (2-way Doppler and range) and landmark observations identified in optical images taken from the on-board cameras.^{10,23)}

The OD setup for each flyover planning cycle was using a short observation interval, of about 9 days, in which many comet's dynamical parameters (gravity, spin axis orientation, landmark coordinates) were fixed, treated as consider parameters with estimated values and uncertainties obtained from the multi-arc OD that was periodically run offline.¹⁸⁾ The acceleration due to the coma drag was modelled using in-situ measurements from ROSINA instrument,¹²⁾ whenever available, or ESOC's engineering coma model,²⁴⁾ estimating scale factor(s) within the OD process, that were subsequently used for manoeuvre optimization and trajectory prediction.

The OD results during the initial flyovers were nominal, obtaining a good fit of all observations and estimating reasonable calibrations for the ΔV of OCMs and WOLs. As expected, with the reductions of pericentre distance, the process got trickier due to the stronger contribution from the higher order terms of the gravitational field to the spacecraft acceleration, requiring, at each planning cycle, much more experimentation with the OD setup until a satisfactory solution would be obtained.

Figure 6 shows the post-fit residuals of the OD performed after flyover#12. The signature around pericentre is a result of the mismodelled acceleration since the short-arc OD did not have enough degrees of freedom in the dynamic models to fit the data. The solution adopted was to strongly deweight the data around pericentre, so that the filter would effectively ignore it, and use the rest of data around apocentre, in particular, the observations from post-flyover manoeuvre to data cut-off to obtain the most accurate estimation of the spacecraft's position and velocity at data cut-off. This implied that the short-arc OD solutions had degraded accuracy for ΔV calibrations and trajectory reconstruction around pericentre. This was not of any concern because the most important use of the each commanding cycle's OD was to generate accurate orbit predictions and, in any case, a full accuracy reconstruction was planned to be performed after the completion of the flyover phase.

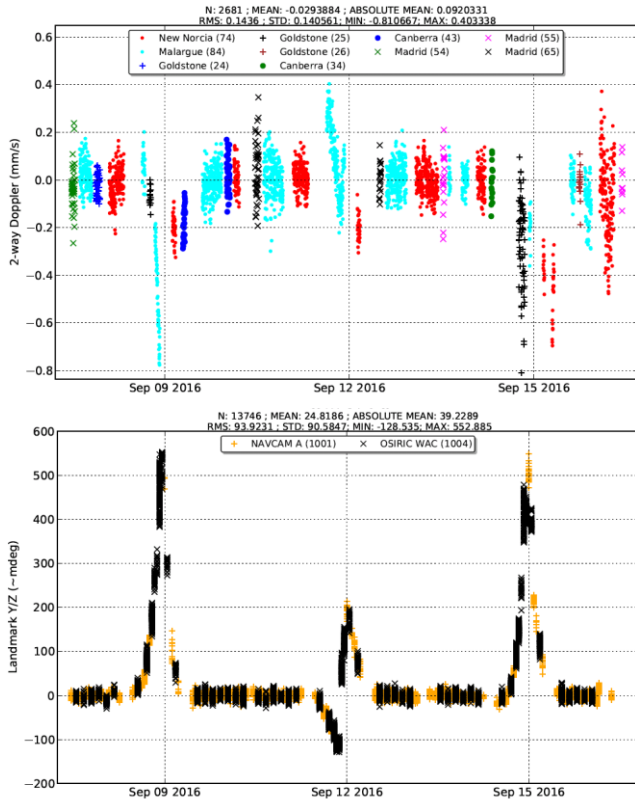


Fig. 6. Post-fit range-rate and landmark (along S/C Y axis) residuals from the OD performed after flyover#12. The signatures during Flyovers #10 and #12 show extremely similar shape, consistent with their similarity in pericentre conditions.

4.6. Manoeuvre Optimization

Rosetta’s manoeuvre computation (and also the trajectory design) was performed using MANTRA, ESOC Manoeuvre and Trajectory Optimization tool,²⁵⁾ that was also used throughout the whole Rosetta mission.

During the flyover phase, the optimization problem to be solved was quite unusual compared to the other mission phases. At each planning cycle, two OCMs had to be commanded: the pre- and post-flyover manoeuvres. The purpose of the OCMs was to control the orbital elements, including radius and time of pericentre. After analysing different setup alternatives, the so-called, “5-manoeuve setup” was selected for actual operations. The optimization arc included the next three pericentres and five OCMs, out of which only the first revolution and first two OCMs were actually commanded at that planning cycle. To improve convergence, the arc was divided in three sub-arcs forcing continuity by matching point constraints.

For the immediately upcoming pericentre it was not possible to impose all the desired flyover conditions because only the pre-flyover manoeuvre could be used to target them. Therefore a minimal set of constraints was used: pericentre radius and, occasionally, the orbital plane tilt. For the subsequent two pericentres in the arc, the full set of conditions was imposed: pericentre radius, latitude and time; orbital plane tilt; and argument of pericentre. This originates an optimization problem with 15 degrees of freedom and 12 (or 11) constraints. The remaining degrees of freedom were used

by the optimizer to minimize fuel consumption, therefore minimizing the size of the manoeuvres. Having small manoeuvres was considered beneficial, not so much because of the fuel saving (which was not a limiting factor for the Rosetta EoM) but because it implied smaller manoeuvre misperformance and therefore better navigation accuracy.

With this approach, Rosetta’s orbit was “loosely controlled” in the sense that only a subset of the desired conditions were actually targeted at the incoming pericentre while the full set was only imposed for the following ones in the arc. This implied that every flyover would be ultimately commanded based on an optimization that targeted only the sub-set of constraints but, as long as the orbit prediction is accurate enough, one would expect that the resulting trajectory would have all the parameters close to the target.

4.7. Navigation Results

The sequence of pericentre radii targeted for the first nine flyovers was: 7.5, 6.7, 6.0, 5.5, 5.0, 4.65, 4.4, 4.05, and 3.9 km. During preliminary analysis, it had been observed that, below 5 km, the gravitational perturbation on the orbital period would start getting very significant. This perturbation is strongly dependent on the actual conditions of the pericentre flown. For the nominal (as targeted) pericentre conditions, it had been noted that the flyover#10 (at about 300 deg longitude) was the one with stronger perturbations.

Table 3 shows a summary of the 15 flyovers flown with reconstructed parameters of interest: difference between actual and nominal pericentre time (21:00 UTC), radius of pericentre (distance from comet’s centre), latitude and longitude of pericentre, osculating argument of pericentre (defined from the terminator plane crossing, night to day), phase angle, and variation of orbital period (as computed by a numerical trajectory propagation using the gravitational model with the final estimates of the 5x5 spherical harmonics).

Table 3. Flyovers’ reconstructed conditions

Peric. #	Date	Δ time [min]	Rp [km]	LAT [deg]	LON [deg]	AOP [deg]	SCP [deg]	Δ OP [h]
1	08/12	-18.9	7.50	19.5	224.9	88.6	70.1	+0.1
2	08/15	-11.2	6.69	20.1	231.1	89.4	70.0	-0.1
3	08/18	-15.8	6.00	20.4	243.2	89.3	70.1	-0.3
4	08/21	0.6	5.50	19.7	245.3	89.1	70.1	-0.7
5	08/24	2.7	5.00	18.8	254.5	88.2	70.1	+0.3
6	08/27	8.7	4.64	17.5	261.9	86.8	70.1	+2.7
7	08/30	8.3	4.41	16.2	272.5	85.5	70.1	+8.5
8	09/02	12.2	4.05	18.2	280.0	85.2	70.1	+19.4
9	09/05	50.3	3.89	8.4	273.2	74.5	70.7	+7.8
10	09/08	107.1	4.09	-0.9	257.2	66.5	71.7	-12.9
11	09/11	77.8	4.09	12.9	277.9	71.4	71.1	+12.4
12	09/14	135.2	4.10	8.6	260.4	68.6	71.5	-4.7
13	09/17	20.0	4.11	20.0	325.9	87.8	70.1	+8.9
14	09/20	20.8	4.10	14.7	338.0	85.3	69.1	+6.1
15	09/23	6.0	4.10	16.4	352.9	83.2	71.0	-8.5

For the first eight flyovers the navigation was very accurate, recording, in flyover#8, a tiny predicted position error of less than 50 m at pericentre. However, it was also the pericentre with stronger gravitational perturbation on the orbital period (+19.4 hours). The predicted variation was about 18.5 hours, thus resulting in an error of 1 hour. This caused that the orbit

phasing errors grew significantly towards the end of the commanded period, reaching an angular difference of 5 degrees. Figure 7 shows the orbit prediction errors per commanded period as the angular difference between the, at the corresponding commanding cycle, predicted spacecraft position vector and the, later, reconstructed position that, for this purpose, can be considered as the one actually flown, given that the reconstruction error is much smaller than the prediction error.

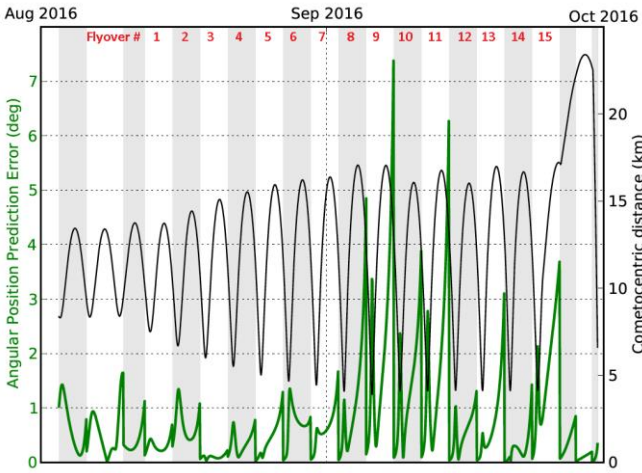


Fig. 7. Angular position prediction error during flyovers

The time of pericentre#9 was shifted about 50 minutes due to the accumulated phasing error. In this flyover the minimum distance of pericentre was reached, 3.9 km from the comet's centre. Even though the total gravitational perturbation was smaller than in #8, a bigger orbital period prediction error was obtained, of about 2 hours, causing the largest orbit prediction error, about 7 degree at the end of the commanded period.

Large orbit prediction errors had two main consequences: (1) since the spacecraft attitude profile is commanded with respect to an inertial reference frame, position prediction error translates to comet pointing error, thus increasing the risk of imaging a portion of the comet fully in the dark; and (2) the time of the following pericentre is advanced or delayed by the error in the predicted orbital period, thus shifting the location of the OCMs in the orbit, and increasing the risk that the spacecraft could not follow the fixed observations schedule.

Given that the navigation errors during flyover#9 were too close to the acceptable limit, it was decided to slightly increase the subsequent pericentre radius to 4.1 km and keep it fixed for the rest of the flyovers. Despite of being slightly higher, similar level of prediction error was obtained in flyovers #10 and #11, recording also significant variations in the pericentre conditions (time, latitude, longitude, argument of pericentre). After flyover#12, the situation slightly improved but, by then, it was too late to attempt any further pericentre reduction because, a few days later, the spacecraft would start the transfer to the initial point of the final descent.

The main driver for the orbit prediction error was the high sensitivity to the estimated position and velocity at data cut-off. A small error at data cut-off (close to apocentre) of less than 10 m in position propagated up to pericentre, resulted in a significantly different gravitational perturbation

on the orbital period that subsequently caused the drift in the orbit phasing. This effect was systematically observed when assessing the orbit prediction accuracy of different orbit determination solutions. The OD performed one day after each planning cycle, with 24 hours of additional observations around apocentre but with data cut-off still before the pre-flyover manoeuvre, was generally much better in predicting the resulting orbital period after the flyover. This would indicate that the estimated gravitational model was doing a good job to model with sufficient accuracy the integrated gravitational perturbations, provided that the predicted trajectory was at the beginning of the flyover close enough to the one actually flown.

4.8. Philae Search

At the beginning of 2016, as soon as the comet's activity allowed flying closer than 20 km, the search for the Philae lander was resumed. In March, May and July 2016, lander search images from OSIRIS-NAC were scheduled mainly during the navigation maintenance slots (allocated for execution of WOLs or acquisition of navigation images). Some of the images showed "candidate landers" that were rejected in subsequent images, while a few of them showed indications of one that could actually be Philae, called "red candidate", very close to the, at that time, best estimate of the location of the lander.^{6,26)} However, an unambiguous high-resolution image of the lander was missing. The very low flyovers during this phase provided a good (and the last) opportunity for the lander search campaign. Nonetheless, it was known that it would not be so straightforward: firstly, the spacecraft was not following a reference trajectory, instead, the orbit was controlled in a "loose way"; secondly, the orbit prediction errors were expected to be quite big, making it extremely difficult to have an equivalent angular error smaller than half the field of view of the camera (about 1.1 deg).

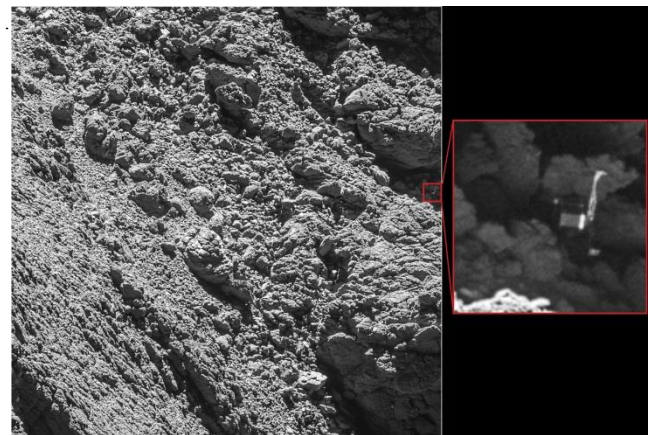


Fig. 8. OSIRIS-NAC image taken on 2016/09/02, showing Philae at rest on its final landing site. Taken at an altitude of 2.7 km, with a resolution of 5 cm/pixel. Copyright: ESA/Rosetta/MPS for OSIRIS Team MPS/UPD/LAM/IAA/SSO/INTA/UPM/DASP/IDA.

Given the (best-guess) trajectory prediction for the whole flyover phase, imaging slots under good illumination and observation conditions of the "red candidate" were identified during flyovers #4 to #9. The first slots were expected, and later confirmed, to have the line-of-sight blocked by a big

“rock” close to the location of the candidate lander. This was likely to improve for the last slots and, fortunately, during flyover #8, the position prediction error around pericentre was so small (less than 50 m error around pericentre) that the red candidate could be captured close to the edge of the image in Fig. 8, clearly showing Philae’s main body and two of its legs and therefore, successfully concluding the lander search campaign.²⁷⁾

5. Final Descent

5.1. Description

Rosetta’s final descent to the comet’s surface was scheduled for September 30th with the main goal of acquiring and transmitting to Earth scientific observations throughout the whole descent, including the highest resolution ones taken immediately before impact.

For the selection of the touchdown area, different alternatives were analysed and evaluated based on illumination conditions, scientific interest and navigation feasibility. The finally selected area was located on the comet’s smaller lobe, in the Ma’at region, next to active pits over 100 m wide and 50 m deep.²⁸⁾ Performing close-up observations of the Ma’at pits was scientifically considered very valuable since its study could help understanding the history of comet 67P.

In terms of navigation, the Ma’at site was more challenging than Agilkia (Philae’s target landing site), because of its much more irregular terrain, being closer to the comet’s CoM (2.0 km, compared to Agilkia’s 2.4 km), and nearby the more than 1-km deep “cliff” that transitions from the comet’s smaller lobe to the “neck” between the two lobes.

5.2. Trajectory Design

The main drivers considered in the design of the descent were: (1) ensure that the spacecraft hits the comet surface in the targeted direction so that the scientific instruments can be pointed towards the impact point; (2) minimize the impact velocity so that the descent duration is longer and the last observation that can be beamed to ground occurs at lower altitude; (3) ensure good illumination conditions of both the Ma’at pits and the actual impact point; (4) keep the spacecraft in the attitude regions such that the HGA can be continuously Earth-pointing to have uninterrupted communications with ground; (5) capability to predict with few-minute-accuracy the actual impact time.

On September 30th 2016, the spacecraft’s one-way light time (time for a signal to travel the distance between spacecraft and ground at the speed of light) was 40 minutes and 2.5 seconds. This prevented any possible intervention from ground to any spacecraft event occurring in the last hours of the descent.

Different strategies were analysed for the descent, mainly related to the inclusion of braking manoeuvre(s) after the collision manoeuvre, which would inject the spacecraft in collision course with the comet. An additional braking manoeuvre would reduce the impact velocity and thus increase the duration of the last part of the descent. However, it would significantly increase the error in the prediction of

the impact time and location, and would interrupt scientific operations and ground communications since the manoeuvre direction was neither compatible with the HGA pointing to Earth nor with the scientific instruments towards the comet.

Considering all this, it was decided to adopt the strategy without braking manoeuvre, and to extend the duration of the whole descent, from collision manoeuvre to impact, so that an additional navigation cycle could be performed on ground shortly after the manoeuvre to obtain a more accurate prediction of the descent trajectory and impact time. Based on this prediction, spacecraft pointing and scientific commands for the last 80 minutes of the descent would be quickly generated and uplinked to perform more accurately the desired scientific observations.

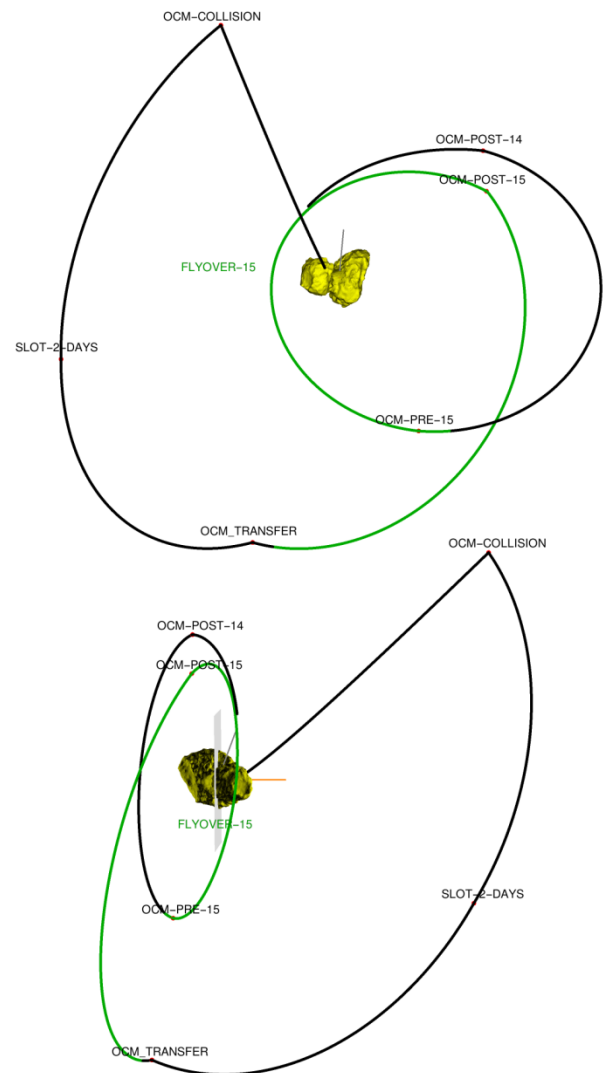


Fig. 9. Rosetta’s trajectory from the last flyover to controlled descent, as seen from Sun (top) and close to the terminator plane (bottom). Marked in green the arc corresponding to the commanded period for flyover#15.

The first stage of the descent trajectory design process was a backward trajectory propagation starting from the desired impact conditions (time, location, impact speed, impact velocity vector parallel to the local normal to the surface) up to a sufficient distance from the comet. Since the descent trajectory was a hyperbolic arc very close to a straight line, certain properties of the initial conditions of the descent could

already be derived (such as latitude, phase angle and initial velocity) without deciding yet the distance of the initial point or, equivalently, the descent's duration. The conditions at touchdown could then be modified until a satisfactory solution was obtained. The second stage of the design was to find a transition from the end of flyover#15, which was fixed in absolute time, to any point of the selected descending trajectory, thus defining the remaining degree of freedom: distance of the initial point of the descent where the collision manoeuvre would be executed. The planned manoeuvres had to be scheduled at times compatible with planning cycles in normal working hours and sufficiently spaced, so that enough radiometric and optical data could be accumulated so that the performance of the previous manoeuvre could be accurately estimated before commanding the upcoming one.

Figure 9 shows the resulting descending trajectory and transfer from the flyover phase. The arc highlighted in green corresponds to the commanded period of flyover#15, for which it was very important to have accurate navigation so that the spacecraft arrived close enough to the reference point where the transfer manoeuvre was to be performed. The selected distance of the initial point of the descent, 23 km from the comet's centre, was mainly a consequence of the design of the transfer arcs to have the proper duration: about 5.5 days from post-flyover#15 to collision manoeuvre. The 14-hour descent duration was considered sufficient to perform the additional planning cycle after the collision manoeuvre.

Another consideration that required further tuning of the trajectory was to ensure, with sufficient margin to account for navigation errors, that the direction of the collision manoeuvre were compatible with the HGA pointing to the Earth. This was achieved by slightly delaying the impact time from the optimal illumination conditions (at 10:20) to the selected nominal impact time: 10:40 UTC. This delay had also the advantage of further improving the illumination conditions of the Ma'at pits at the time of the planned scan that would take place around 1 hour before impact.

In summary, the choices for the available degrees of freedom in the trajectory design were: target impact coordinates tuned to minimize the chances of impact in a non-illuminated area; impact time chosen to optimize the illumination conditions and ensure HGA coverage; minimized impact speed (90 cm/s) while ensuring a sufficiently high descent's initial speed (33 cm/s); and the comet-fixed velocity at impact aligned with the local normal to the surface.

5.3. Planning Cycles

Table 4 lists the planning cycles and manoeuvres performed from the last flyover to the final descent and impact. The turnaround time, defined as the elapsed time from data cut-off to the start of execution of the new commands on-board, had to be progressively reduced from the 27h of the flyover phase to the extremely compressed 8 hours of the last commanding cycle of the mission. This means that, after subtracting the roundtrip light-time (1h 20 min), only 7 hours were available on ground for the completion of the full planning cycle described in Section 4.3, with the simplification that only a handful of commands were required to update the spacecraft attitude profile for the last 80 minutes of the mission.

Cycle Name	Data cut-off	Start CMDs	OCM Name	OCM Date
Flyover #15	09/22 04:00	09/23 06:40	Pre#15	09/23 09:00
			Post#15	09/24 09:00
Transfer #1	09/25 04:00	09/26 06:40	Transfer	09/26 09:00
Transfer #2	09/27 04:00	09/28 00:00	Slot-2-days	09/28 02:20
Impact #1	09/29 04:30	09/29 18:30	Collision	09/29 20:50
Impact #2	09/30 01:00	09/30 09:20	-	-

5.4. Navigation Analysis

In order to assess the targeting accuracy of the descent strategy (in terms of impact location and time), Monte Carlo simulations were run, propagating the trajectory up to the intersection with the comet shape model, emulating what would happen in reality. The initial state vector was taken at the time of data cut-off of the planning cycle, "Impact #1", that commanded the collision manoeuvre. The level of perturbations used, listed in Table 5, was defined in a conservative manner, so that the maximum expected dispersion could be obtained.

Parameter	Probability Distribution	Sigma / interval half length
Initial Position (radial, along, cross-track)	normal	(50, 20, 20) m
Initial Velocity (radial, along, cross-track)	normal	(1, 0.5, 0.5) mm/s
Collision Manoeuvre ΔV (magnitude, direction error)	uniform	(7 mm/s, 0.7 deg)
Coma drag	normal	100 % of nominal acc.
Solar Radiation Pressure	normal	5 % of nominal acc.
CG Gravity GM	normal	1 % of nominal value
CG CoM (x,y,z)	normal	(3, 3, 7) m
CG Gravity Coeff. Deg 2	normal	10 % of nominal value plus 0.001 noise
CG Gravity. Coeff. Deg 3	normal	20 % of nominal value plus 0.005 noise
CG Gravity Coeff. Deg 4,5	normal	50 % of nominal value plus 0.001 noise

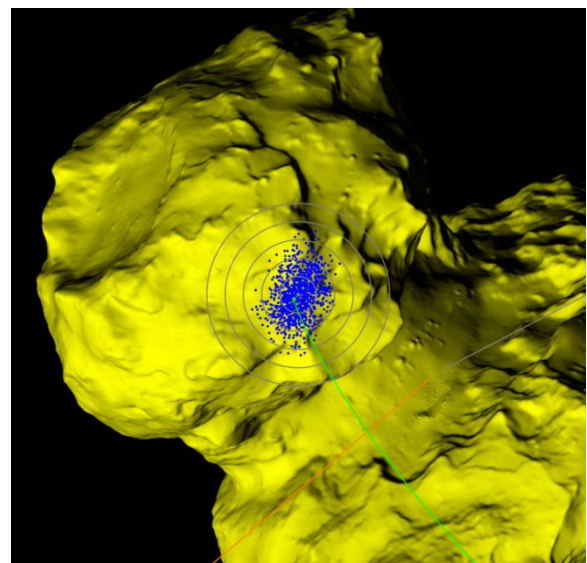


Fig. 10. Landing dispersion results from the Monte Carlo analysis.

The resulting impact points are represented in blue in Fig. 10, where the concentric circles around the target point (marked in grey) are spaced by 100 m in radius. The obtained maximum dispersion was 350 m in impact location and 15 minutes in impact time. The results from this analysis were used to tune the coordinates of the target impact point to minimize the likelihood of impacting on a non-illuminated location and also to define the strategy for the spacecraft attitude profile during the descent based on the resulting covariance of the spacecraft position at certain stages of the descent.

5.5. Navigation in the Transition Arcs

After the execution of the post-flyover#15 manoeuvre the spacecraft abandoned the challenging close distances to the comet and the navigation accuracy came back to the level that had been achieved in the previous mission phases. The main driver for the prediction error was again the manoeuvre misperformance and no longer the OD accuracy. The significant signatures in the observation residuals were no longer obtained and thus no special observation weighting scheme was needed anymore.

As an output of the impact design, a reference trajectory had been generated and used to plan the activities during the descent. The OCMs during the transition arcs were commanded to target the comet-fixed coordinates of the initial point of the descent obtained from the reference trajectory. In this way the actual trajectory would be brought as close as possible to the reference, making sure that all previous analysis would still be applicable. This was especially important to ensure that the HGA could be continuously pointing to Earth from collision manoeuvre to impact.

Once the performance of the transfer manoeuvre (10.4 cm/s) was assessed, it was observed that the spacecraft would arrive to the initial point of the descent with about 1 km position error, pulling the direction of the collision manoeuvre close to the HGA limit. To avoid any unnecessary risk, it was therefore decided to use the stochastic manoeuvre slot, two days before impact, to trim the navigation errors with a ΔV of 7 mm/s. After this, the spacecraft arrived with very small navigation errors to the initial point of the descent. The collision manoeuvre (34.6 cm/s) was computed to impact at the target time and on the target point (defined by its comet-fixed coordinates), letting free the impact velocity that hardly differed from the desired conditions due to the small error in the initial point.

5.6. Navigation Cycle after the Collision Manoeuvre

The orbit determination for the last planning cycle of the mission had continuous 2-way Doppler and range measurements throughout the manoeuvre and during the (initial part of the) descent. In the arc before the collision manoeuvre, one navigation image per hour was acquired. After the manoeuvre, five NAVCAM images were taken, from 23:00 to 01:00, the last ones of the mission. One OSIRIS-WAC image taken at 01:22 (with the spacecraft at 17 km from the comet's centre) arrived just in time to be processed and it was included in the orbit determination. The manoeuvre was extremely accurate: slight over-performance of 1.1 mm/s (+0.4%) and a direction error of less than 0.1 deg.

The trajectory propagation up to intersection with the shape model resulted in a predicted impact time of 10:38:32, 44 metres away from the target point.

Afterwards, the only task left on ground was to monitor the spacecraft telemetry and to perform periodic ODs as more radiometric data and OSIRIS-WAC images were acquired to assess that the spacecraft was in the right path. In each subsequent OD solution, the impact time was progressively delayed. The last solution, performed in real time during the descent, predicted the impact at 10:39:08, 34 m away from the target.

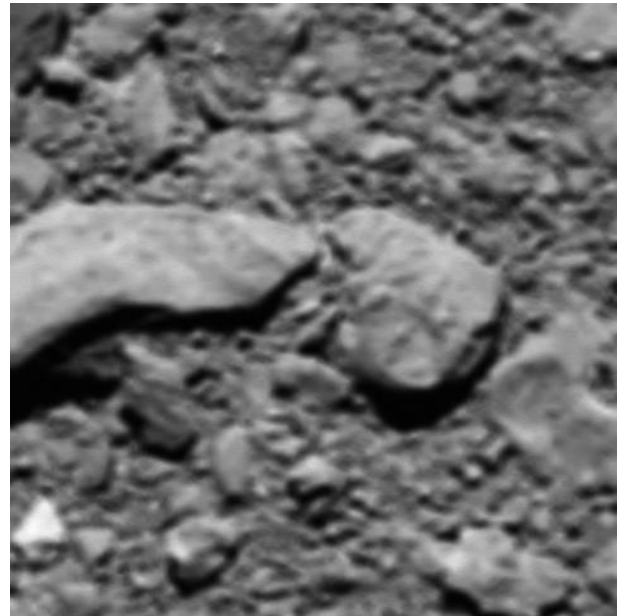


Fig. 11. Last image transmitted by Rosetta, taken with OSIRIS-WAC at ~20 m altitude, measuring ~1m across, with a resolution of 2 mm/pixel.

Copyright: ESA/Rosetta/MPS for OSIRIS Team
MPS/UPD/LAM/IAA/SSO/INTA/UPM/DASP/IDA

5.7. Final Descent Reconstruction

During the descent, the spacecraft successfully performed all the planned activities until loss of signal on ground due to HGA de-pointing at impact. Figure 11 shows the last image transmitted by Rosetta shortly before impact. The last spacecraft's telemetry packet received on ground had a time tag of 11:19:36.5 UTC, which, subtracting the one-way light time, implied that the impact had occurred at 10:39:34 UTC, 26 seconds earlier than the target time.

After the event, all OSIRIS images taken during the descent could be analysed to accurately determine the actual impact point that happened to be 33 metres away from the target, very close to the latest predictions. The last image in which navigation landmarks were identified was taken at 10:07:18 UTC, at an altitude of about 1.5 km. A final trajectory reconstruction was then performed, by constraining the OD to impact in the reconstructed location at the reconstructed time.

6. Conclusion

The Rosetta End of Mission phase was considered a full success despite being extremely challenging. All operations could be conducted successfully, managing to safely fly the

spacecraft very close to the comet's surface and to the actual navigation limit, defined either by star tracker performance or navigation accuracy. All this was achieved without endangering the mission safety, even though higher risks were assumed, which for previous mission phases were considered unacceptable.

The landing trajectory was extremely accurate (33 metres impact location and 24 seconds impact time away from the targets) and fulfilled all scientific goals: close-up observations of the Ma'at pits and Rosetta's highest resolution image of the surface of the comet.

References

- 1) Morley, T. and Budnik, F., "Rosetta Navigation at its First Earth Swing-by", Proceedings 19th International Symposium on Space Flight Dynamics - 19th ISSFD, Kanazawa, Japan, 2006.
- 2) Budnik, F. and Morley, T., "Rosetta Navigation at its Mars Swing-by", Proceedings 20th International Symposium on Space Flight Dynamics - 20th ISSFD, Annapolis, USA, 2007.
- 3) Morley, T. and Budnik, F., "Rosetta Navigation for the Fly-by of Asteroid 2867 Šteins", Proceedings 21st International Symposium on Space Flight Dynamics - 21st ISSFD, Toulouse, France, 2009.
- 4) Morley, T., et al., "Rosetta Navigation for the Fly-by of Asteroid 21 Lutetia", Proceedings 23rd International Symposium on Space Flight Dynamics - 23rd ISSFD, Pasadena, USA, 2012.
- 5) Morley, T., et al., "Rosetta Navigation from Reactivation Until Arrival at Comet 67P Churyumov-Gerasimenko", Proceedings 25th International Symposium on Space Flight Dynamics – 25th ISSFD, Munich, Germany, 2015.
- 6) Muñoz, P., et al., "Rosetta Navigation During Lander Delivery Phase and Reconstruction of Philae Descent Trajectory and Rebound", Proceedings 25th International Symposium on Space Flight Dynamics - 25th ISSFD, Munich, Germany, 2015.
- 7) "Rosetta Mission Extended", ESA, http://www.esa.int/Our_Activities/Space_Science/Rosetta/Rosetta_mission_extended
- 8) Antreasian P.G., et al., "The design and navigation of the NEAR-Shoemaker landing on Eros", AAS/AIAA Astrodynamics Specialist Conference, Quebec, Canada, 2001.
- 9) Accomazzo, A., et al., "The final year of the Rosetta mission", Acta Astronautica, Volume 136, July 2017, pp. 354-359.
- 10) Muñoz, P. et al., "Preparations and Strategy for Navigation during Rosetta Comet Phase", Proceedings 23rd International Symposium on Space Flight Dynamics - 23rd ISSFD, Pasadena, USA, 2012.
- 11) "Rosetta Safe Mode 5 Km from Comet", ESA, <http://blogs.esa.int/rosetta/2016/05/30/rosetta-safe-mode-5-km-from-comet/>
- 12) Balsiger, H., et al., "Rosina – Rosetta Orbiter Spectrometer for Ion and Neutral Analysis", Space Science Reviews, February 2007, Volume 128, Issue 1, pp 745-801.
- 13) "Krypton and Xenon Added to Rosetta's Noble Gas Inventory", ESA, <http://blogs.esa.int/rosetta/2016/06/14/krypton-and-xenon-added-to-rosettas-noble-gas-inventory/>
- 14) Keller, H.U., et al., "OSIRIS - The Scientific Camera System Onboard Rosetta", Space Science Reviews 128,433–506, 2007.
- 15) Pardo de Santayana, R., and Lauer, M., "Optical Measurements for Rosetta Navigation near the Comet", Proceedings 25th International Symposium on Space Flight Dynamics - 25th ISSFD, Munich, Germany, 2015.
- 16) Castellini F., et al., "Optical Navigation for Rosetta operations near comet Churyumov-Gerasimenko", AAS/AIAA Astrodynamics Specialist Conference, Hilton Head, SC, USA, 2013.
- 17) Pardo de Santayana R., et al., "Surface Characterization and Optical Navigation at the Rosetta Flyby of Asteroid Lutetia", Proceedings 24th International Symposium on Space Flight Dynamics - 24th ISSFD, Laurel, USA, 2014.
- 18) Godard, B., et al., "Multi-arc Orbit Determination to determine Rosetta trajectory and 67P physical parameters", Proceedings 26th International Symposium on Space Flight Dynamics – 26th ISSFD, Matsuyama, Japan, 2017.
- 19) Guilanyà, R., Companys, V., "Operational Approach for the ExoMars Aerobraking", Proceedings 23rd International Symposium on Space Flight Dynamics - 23rd ISSFD, Pasadena, USA, 2012.
- 20) Werner, R.A., Scheeres, D.J., "Exterior gravitation of a polyhedron derived and compared with harmonic and mascon gravitation representations of asteroid 4769 Castalia". Celestial Mechanics and Dynamical Astronomy, 1996, vol. 65, no 3, p. 313-344.
- 21) ESOC FD NAVCAM Shape Model, ESA, http://imagearchives.esac.esa.int/index.php?page/navcam_3d_model
- 22) Budnik, F., et al., "ESOC's System for Interplanetary Orbit Determination", ESA SP-548, 387-392, 2004.
- 23) Godard, B. et al., "Orbit Determination of Rosetta Around Comet 67P Churyumov-Gerasimenko", Proceedings 25th International Symposium on Space Flight Dynamics – 25th ISSFD, Munich, Germany, 2015.
- 24) Bielsa, C., et al., "Operational Approach for the Modelling of the Coma Drag Force on Rosetta", Proceedings 24th International Symposium on Space Flight Dynamics, 24th ISSFD, Laurel, USA, 2014.
- 25) Schoenmaekers J., et al., "MANTRA - Flight Dynamics Interplanetary Manoeuvre Optimisation - Software Specification Document", ESOC, issue 2, Rev 15, Darmstadt, Germany, 2015.
- 26) Biele, J., et al., "The landing(s) of Philae and inferences about comet surface mechanical properties", Science, 31 July 2015: Vol. 349 no. 6247. DOI: 10.1126/science.aaa9816.
- 27) "The story behind finding Philae", ESA, <http://blogs.esa.int/rosetta/2016/09/28/the-story-behind-finding-philae/>
- 28) Vincent, J.B., et al., "Large heterogeneities in comet 67P as revealed by active pits from sinkhole collapse". Nature, 2015, 523(7558), 63-66.